Is the nitrogen recombination determinant in the titania thin films crystallization deposited with a microwave axial injection torch?

A. Perraudeau, C. Dublanche-Tixier, C. Chazelas, P. Tristant
Université de Limoges, CNRS, IRCER, UMR 7315, F-87000, France.

Abstract: An atmospheric pressure PECVD system using an axial injection torch was used to deposit TiO_2 films on Si substrates. Depending on the process parameters, two different coating growth mechanisms were observed. Optical emission spectroscopy analyses were carried out for a better understanding of the plasma chemistry. It was possible to draw hypotheses on the process parameters to limit homogeneous nucleation during deposition and promote growth by surface reaction to obtain a crystallized thin film.

Keywords: Optical emission spectroscopy, axial injection torch, AP-PECVD, TiO_2

1. Introduction

Titanium dioxide is widely studied nowadays. Its high band gap, around 3 eV, makes it suitable for many applications as photocatalysis, hydrogen production or photovoltaic cells [1–3]. The classic sol-gel synthesis route [4] is more and more replaced by processes like chemical vapor deposition (CVD) [5], plasma enhanced CVD (PECVD) [6] or sputtering systems [7]. However, these processes usually operate at low pressure (from 0.1 to 100 Pa) and thus require substrate heating, most of the time exceeding 400°C. Low-temperature solutions were investigated in the past few years such as atmospheric pressure PECVD (AP-PECVD) systems [8–10]. Their versatility and low-cost make them interesting for the oxide thin film deposition. However, at atmospheric pressure, more collisions are generated between reactive species in the plasma phase. Before reaching the substrate, they can react and create clusters by homogeneous reactions. These powders are transported to the substrate and can interfere with the film growth and be embedded in the layer. This phenomenon is amplified when precursor partial pressure and/or plasma power are increased. This phenomenon should be avoided to deposit homogeneous nonpolluted coatings.

In this study, an axial injection torch was used for titania deposition. Optical emission spectroscopy (OES) measurements were conducted to get a better understanding of the plasma, then different conditions of deposition were selected and the microstructure of the as-deposited films were characterized and discussed.

2. Experimental

a. The axial injection torch (TIA)

The AP-PECVD system using an axial injection torch used in this study is presented in Fig.1. Microwaves are provided by a SAIREM 1200 KED generator (2,45 GHz) and transported by a rectangular waveguide to supply the cylindrical outer conductor of the coaxial guide. The nozzle, with a 2 mm inner diameter, is placed on the top of the coaxial conductor in a large cylindrical open-air reactor. An exhaust device removes gas or particles produced during the deposition. The substrate holder faces the plasma jet and can be moved along the *x* and *y*-axis using a Labview® program. Its height can be changed manually.

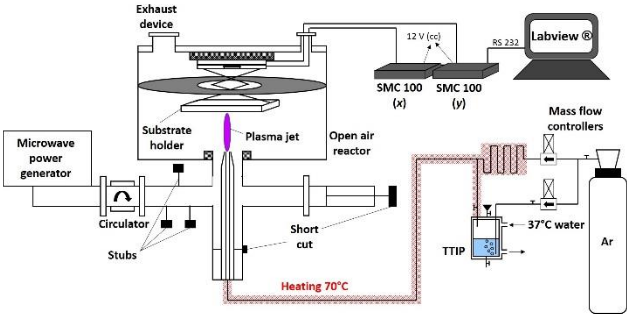

Fig.1. Schematic representation of the AP-PECVD microwave plasma torch.

Argon (AirLiquide Alphagaz I, purity >99.999%) was used as plasma gas. Oxygen required to form titania films was mainly provided by the ambient air. The titanium tetraisopropoxide (TTIP), organometallic precursor (Alfa Aesar, $Ti(OC_3H_7)_4$, purity >97%) was kept into a 300-mL container under argon atmosphere, heated at a constant temperature of 37°C. Argon gas bubbled into the container and went out saturated with TTIP into the stainless steel gas lines, maintained at a temperature of 70°C to avoid the precursor vapor condensation during the transport. The TTIP flow rate was fixed by the argon flowrate bubbling into the container. The plasma gas and the carrier gas were mixed in the lines and transported through the inner conductor of the coaxial line to reach the nozzle. Parts of (100) monocrystalline silicon wafers were used as substrates. They were cleaned before coating with an optical paper and ethanol.

In this study, the incident microwave power was set to 420 W to ensure plasma stability during deposition, but low enough to limit homogeneous nucleation. The distance between the nozzle and the substrate can be adjusted to optimize the residence time of the species into the plasma to avoid the formation of powder in the gas phase. The gas flow rates appeared to have a strong influence on the coating growth and the particles formation in the plasma. The argon plasma flow rate ensures discharge stability and the precursor dilution in the plasma phase. It has to be sufficient to obtain a stable jet and promote the film growth instead of the formation of non-adherent powder. It was set in this study at 17 slpm. The TTIP flow rate is determinant for the thin film growth and was fixed at 0.2 slpm to limit homogeneous nucleation and promote a film growth by surface reaction.

b. Optical emission spectroscopy

The plasma jet was analyzed by optical emission spectroscopy using an Acton SectraPro® SP-2750 (Princeton Instruments). Its focal length is 750 mm, and a 1800 groove/mm grating was used. The entrance slit width was kept at 40 µm for all the analyses. The CCD (Charge Coupled Device) camera used is a PIXIS 400B_eXcelon, with a 1340 x 400 detector matrix and its pixel size is 20 x 20 µm².

Investigations were carried out by focusing on a "slice" of the plasma at the entrance slit of the monochromator. Each slice was defined by the z coordinate targeted. The excitation temperature T_{exc} was then determined by the Boltzmann plot method (Fig.2) by using the following equation:

$$\ln\left(\frac{I_{ij}\lambda_{ij}}{g_i A_{ij}}\right) = -\frac{E_i}{kT_{exc}} + C \qquad (1)$$

where I_{ij} is the measured relative intensity (in arbitrary units) of the emission line between the energy levels i and j, λ_{ij} its wavelength, g_i is the statistical weight of the emitting upper level i of the considered transition, and A_{ij} is the transition probability for spontaneous radiative emission from the level i to the lower level j. Finally, E_i is the energy of the level i, k is the Boltzmann constant, and C is constant. The spectroscopic data (E_i, λ_{ij}, A_{ij}, g_i) are extracted from the NIST database.

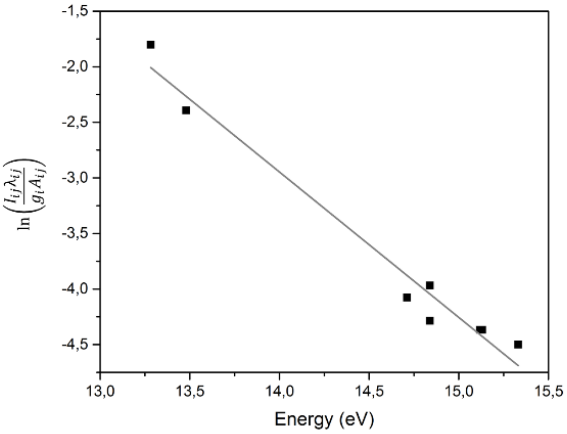

Fig.2. Boltzmann plot using Ar emission lines corresponding to z = 5 mm and a power of 420 W.

It is then possible to determine the atomic density ratios of N, O and Ti with Ar as the reference with the equation:

$$\frac{N_X}{N_Y} = \frac{I_X.\lambda_X.A_Y.g_Y.Z_X(T_{exc})}{I_Y.\lambda_Y.A_X.g_X.Z_Y(T_{exc})}\exp\left(\frac{E_X - E_Y}{k.T_{exc}}\right) \qquad (2)$$

where NX and NY are the relative atomic densities of X and Y, respectively, X and Y representing the associated emission lines of the atomic species. Z corresponds to the partition function of the considered emitting species, depending on the excitation temperature.

c. Thin films characterization

First, the morphologies of the titania films were observed using a field emission scanning electron microscope (FESEM) LEO 1530 VP (ZEISS) with an operating range of 5 kV. A 5-nm platinum coating covered the analyzed surfaces before observations. X-Ray diffraction (XRD) was used to determine the crystallinity of the films. The apparatus is a D8 Advance (Bruker), with a θ-2θ configuration using the Cu Kα filtered radiation (0.154 nm). The measurements were performed between 20° and 60°, and the sample was spinned at 15 rpm.

3. Results

a. Optical emission spectroscopy investigation

Investigations were first performed on a plasma jet without precursor injection for the excitation temperature calculations (Fig.3). Then, it was verified that the TTIP injection did not changed significantly its value.

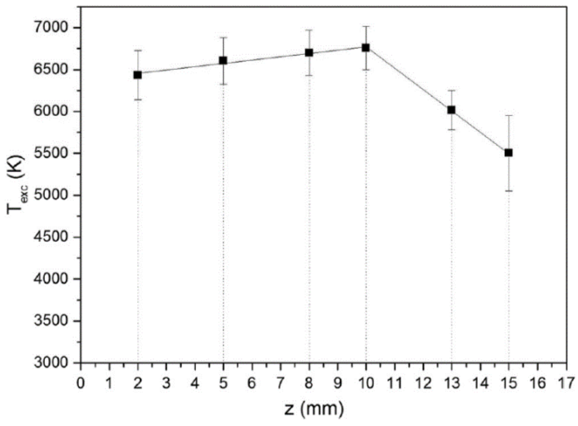

Fig.3. Excitation temperature profile as a function of z [11].

The relative atomic densities of Ti [11], N and O were estimated and are presented in Fig.4 and Fig.5. It appears that air entrainment in the plasma jet is efficient considering that oxygen and nitrogen molecules are decomposed since z = 5 mm (Fig.5).

Fig 4 shows from z = 2 mm to 11 mm the Ti concentration which tends to increase by a factor of approximately 5. This trend could be interpreted as a progressive decomposition of TTIP along the ionizing region (i.e., the dart), due to electron collisions as well as thermal effects. This is consistent with the fact that in this region, when z increases, both electron temperature and density also increase (Fig.3). From z = 10 mm to 15 mm (i.e., in the plume), however, Fig. 4 shows that the Ti rate decreases abruptly by a factor of about 50, indicating recombination of the atomic titanium.

Thus, for a given set of parameters, it may probably exist a distance d_1 before the Ti depletion where homogeneous nucleation could be limited.

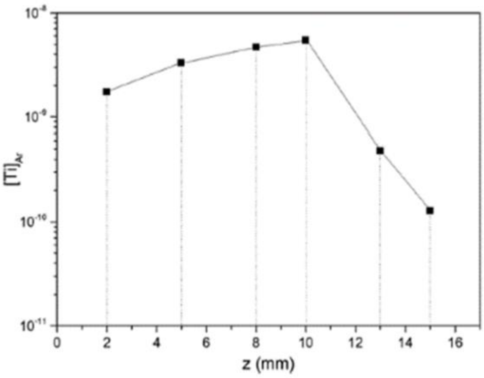

Fig.4. Spatially resolved Ti relative concentration in the discharge as a function of z [11].

Fig.5 shows that oxygen ($^5S_2 \leftarrow ^5P_{3,2,1}$) increases along the plasma to reach a maximum relative atomic density at z = 10 mm. Then it slightly decreases, which could be the evidence of the dioxygen recombination beginning, following the reaction:

$$O + O \rightarrow O = O \qquad (5{,}1\ \text{eV}) \qquad (3)$$

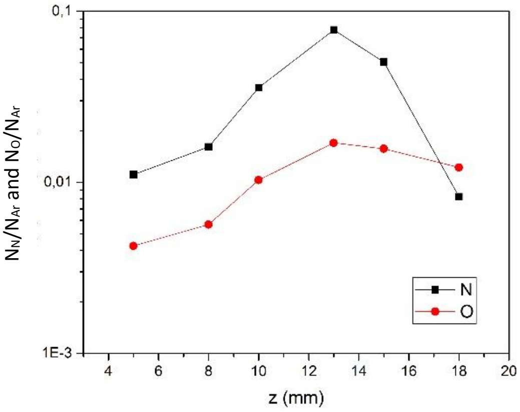

Fig.5. Oxygen and nitrogen relative atomic density profiles as a function of z.

Fig.5 also displays the N ($^4P_{1/2,\ 3/2,\ 5/2} \leftarrow ^4S_{3/2}$) relative density profile. The curve reaches a maximum at z = 13 mm and then a hard decrease beyond z = 15 mm. As for O, it could be the evidence of nitrogen exothermic recombination, as follow:

$$N + N \rightarrow N \equiv N \qquad (9{,}8\ \text{eV}) \qquad (4)$$

Thus, it may exist probably, for given operating parameters, a distance d_2 where the energy released by the recombination of O and/or N energy could be absorbed by the film to crystallize.

b. TiO_2 films on silicon wafers

Fig.6 presents the surfaces of the titania films elaborated at different nozzle-substrate distances. At a working distance of 10 mm (Fig.6a), the film exhibits a rice-like surface, typical of a columnar structure composed of aligned TiO_2 crystals and displaying an intercolumnar porosity [12]. At nozzle-substrates distances of 13 and 15 mm (Fig.6b and Fig.6c, respectively), the coatings surfaces are composed of roundish agglomerated particles, as a cauliflower-like structure.

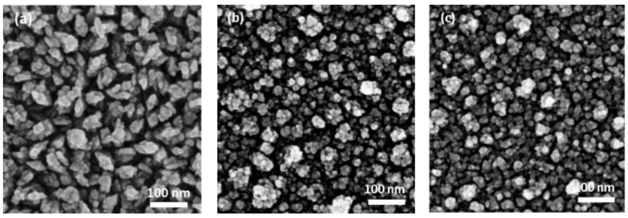

Fig.6. FESEM image of the TiO_2 films elaborated at different nozzle-substrates distances: (a) 10 mm, (b) 13 mm and (c) 15 mm.

From the two morphologies observed, two growth mechanisms can be deduced. Fig.6a is characteristic of a growth by surface reaction. Reactive species reach the substrate and the film is grown by chemical surface reaction. Fig.6b and Fig.6c are typical of growth by nanoparticles agglomeration. Homogeneous nucleation happens in the gas phase and creates particles that will then be glued as cauliflower-like columns.

As suggested before (Fig.4), it indicates that for a given set of parameters, there is a distance underneath which surface reaction is promoted instead of agglomeration of particles originating from homogeneous nucleation.

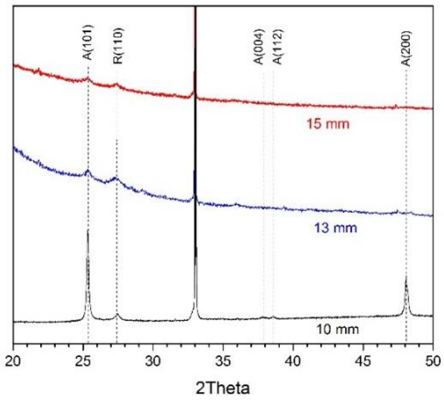

Fig.7. XRD patterns of titania films elaborated at different substrate-nozzle distances.

Fig.7 displays de XRD patterns obtained for the films elaborated at different nozzle-substrate distances. When the substrate-nozzle distance was increased, the film becomes less crystallized. Different hypothesis could be mentioned to explain this phenomenon. Firstly, the substrate is out of the hot part of the plasma jet, and thus there is less heat transferred to the growing film. Secondly, atomic species, like N or O, in the plasma are recombined releasing energy which can be used afterward to crystallize the coating, depending on the position of the substrate; if the substrate is out of the recombination zone, the film is not well-crystallized and could become amorphous. As suggested previously (Fig.5), it exists an optimal distance where the film could gather the recombination energy to crystallize.

4. Conclusions

Depending on the process parameters, it was possible to obtain crystallized TiO_2 coatings, displaying two different morphologies. Two corresponding growth mechanisms were highlighted and linked to the plasma chemistry. It seems indeed possible to find a nozzle-substrate distance where surface reaction is promoted instead of homogeneous nucleation.

At a given nozzle-substrate distance, the TiO_2 film was not well-crystallized. It seemed to correspond to a distance where O and N hardly decrease in the plasma, thus their recombinations had already happened. Further investigations are necessary to confirm this tendency and that the recombination energy of these species participates in the film crystallization.

In the ideal conditions, if the recombination distance d_1 and the homogeneous nucleation limit d_2 are overlapped, the resulting film should grow by surface reaction and not be polluted by powders created in the plasma phase.

The main challenge is then to modulate the process parameters to deposit crystallized coatings on thermally sensitive substrates.

5. Acknowledgments

The authors would like to gratefully acknowledge financial support granted by the Region Limousin and the laboratory of excellence ∑-Lim.

6. References

[1] S. Collette *et al.*, Surf. Coat. Technol., **289**, (2016).

[2] X. Chen *et al.*, Chem. Rev., **107**, (2007).

[3] M. Salado *et al.*, Nano Energy, **35**, (2017).

[4] A.M. Gaur *et al.*, Lect. Notes Eng. Comput. Sci., **2191**, (2011).

[5] R. Tu *et al.*, Mater. Trans., **49**, (2008).

[6] K.L. Choy, Prog. Mater. Sci., **48**, (2003).

[7] R. Alvarez *et al.*, Phys. Status Solidi A., **210**, (2013).

[8] R. Maurau *et al.*, Surf. Coat. Technol.,**232**, (2013).

[9] N.D. Boscher *et al.*, Appl. Surf. Sci., **311**, (2014).

[10] H. Fakhouri *et al.*, J. Phys. Appl. Phys., **47**, (2014).

[11] Y. Gazal *et al.*, J. Appl. Phys., **121**, (2017).

[12] Y. Gazal *et al.*, Thin Solid Films, **600**, (2016).